Available online at www.sciencedirect.com
SCIENCE DIRECT®
International Journal of Heat and Mass Transfer 47 (2004) 4601–4614
International Journal of HEAT and MASS TRANSFER
www.elsevier.com/locate/ijhmt

Development of gas–solid direct contact heat exchanger by use of axial flow cyclone

Akihiko Shimizu [a,*], Takehiko Yokomine [a], Tatsuro Nagafuchi [b]

[a] *Interdisciplinary Graduate School of Engineering Sciences, Kyushu University, 6-1 Kasuga-kouen, Kasuga-shi, Fukuoka 816-8580, Japan*

[b] *Miura Co., Ltd., 7 Horie-cho, Matsuyama-shi, Ehime 799-2696, Japan*

Received 16 May 2003; received in revised form 8 August 2003
Available online 25 June 2004

Abstract

A heat exchanger between particulate or granular materials and gas is developed. It makes use of a swirling gas flow similar to the usual cyclone separators but the difference from them is that the swirl making gas is issued into the cyclone chamber with downward axial velocity component. After it turns the flow direction near the bottom of the chamber, the low temperature gas receives heat from high temperature particles supplied from above at the chamber's center. Through this configuration, a direct contact and quasi counter-flow heat exchange pattern is realized so that the effective recovery of heat carried by particles is achieved. A model heat exchanger was manufactured via several numerical experiments and its performances of heat exchange as well as particle recovery were examined. Attaching a small particle diffuser below the particle-feeding nozzle brought about a drastic improvement of the heat exchange performance without deteriorating the particle recovery efficiency. The outlet gas temperature much higher than the particle outlet temperature was finally obtained, which is never realized in the parallel flow heat exchanger.

Keywords: Gas–solid heat exchanger; Axial flow cyclone; Direct contact; Counter flow heat exchanger

1. Introduction

Voluminous amount of high temperature particulate or granular materials appear in some conventional engineering processes such as steel manufacturing, chemical engineering and cement production. Pressurized fluidized bed coal combustion (PFBC) or waste combustion produces hot fly ash steadily. In most cases, the thermal energy carried by hot particles is only an object of cooling and is abandoned without being used after respective processes. If a suitable means of recovering it becomes available, it will contribute to energy saving, though the relative amount of heat carried by particles is usually small compared to the total heat generation of the respective equipments.

Meanwhile, situations can exist in which relative amount of heat carried by solid particles is not necessarily small. In several conceptual designs of fusion power reactors, the possibility of gas–solid suspension cooling is examined as a promising alternative to the simple helium cooling [1,2]. One of such concepts is illustrated in Fig. 1. Suspended particles can improve the inherent poor heat transfer characteristics of the single-phase gas through increased heat capacity, additive turbulence production and their roles of emitting/absorbing thermal radiation and these features are appropriate for the cooling of extremely high heat flux components such as first wall or diverter plate the heat flux of which is expected to reach up to several megawatt per square meter. However, though even slight solid

* Corresponding author. Tel./fax: +81-92-583-7601.
E-mail address: shimizu@ence.kyushu-u.ac.jp (A. Shimizu).

0017-9310/$ - see front matter
doi:10.1016/j.ijheatmasstransfer.2003.10.045

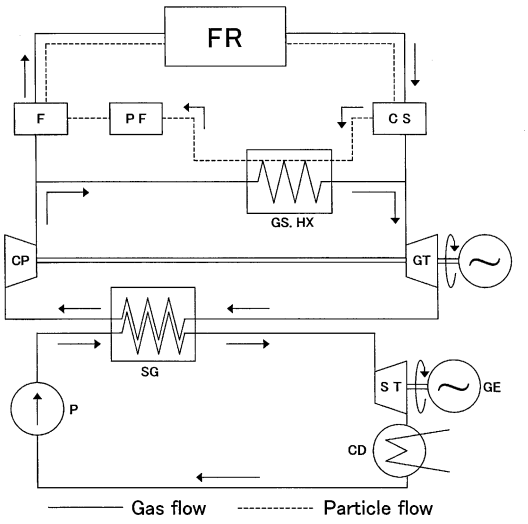

Fig. 1. Concept of suspension-cooled fusion power reactor system.

loading can fairly improve the heat transfer, a suspension with substantial loading will be required to cope with such a high heat flux. If so, because it is unrealistic to feed the heavily loaded suspension directly into the gas turbine due to blade erosion, the suspended particles must be separated from the coolant before it enters the turbine. On the other hand, the thermal output from the reactor is carried, for the heavily loaded suspension, mainly by solid phase, its ratio being equals to the thermal mixing ratio Γ_{th} i.e. the ratio of heat capacity flow rate of solid to that of gas, which is usually of the same order as the mass mixing ratio, i.e. the ratio of mass flow rates of both phases. Then, the thermal energy retained in separated solid should be recovered and fed back to the flow somewhere upstream above the turbine in order to realize an effective energy conversion system.

2. Counter-flow gas–solid heat exchanger

The key is, therefore, the heat exchanger between hot particles as a primary flow and gas as a secondary flow. The simple cooling of particulate material is easy because of its large specific surface area. For instance, if high temperature particulate material is mixed with low temperature gas and then they are separated again, the solid and gas of the same intermediate temperature remain, the result being equivalent to that of a parallel flow heat exchanger between them. The effective recovery of thermal energy can only be realized by the counter-flow type heat exchanger in which outlet temperature of the secondary flow can be raised above that of the primary flow. However, the counter-flow heat exchanger between gas and slowly moving particulate material with separating wall in between is not effective because two heat transfer phenomena, one the convection between separating wall and gas flow and the other the apparent conduction within quasi-packed bed, are both poor, as shown in (a) of Fig. 2. The effective heat exchange is realized only when solid particles and gas contact each other directly in the counter-flow, as schematically illustrated in (b) of Fig. 2. One possibility is to let the hot particles fall freely in vertically upward gaseous flow. However, it is apparent that unless upward gaseous velocity is less than particle's free-fall terminal velocity, the particles fly away with gas. The heat exchanger with such a small gaseous velocity would have an exorbitant size.

The problem is, then, how to realize a flow field in which apparent body force that acts on particles becomes large compared to gravity and adapting a swirling flow field like centrifugal separators is the natural con-

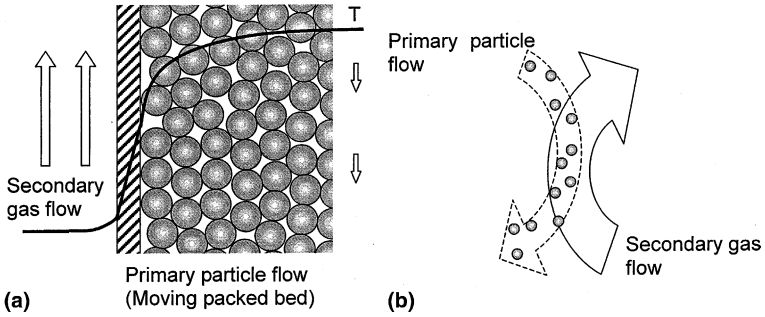

Fig. 2. Types of counter-flow heat exchanger between gas and solid: (a) counter flow with separating wall; (b) direct contact counter flow.

clusion. In addition, the particles must be recovered effectively after giving heat to the gas. These considerations led the authors to the concept of gas–solid direct contact heat exchanger by use of the cyclone.

3. Structure of developed heat exchanger

Based on above, a series of trial and error was performed to search an optimum shape of the heat exchanger via numerical simulations in which various types of gas/solid feeding were tested. One example is shown in Fig. 3 in which hot particles are fed downward into the chamber from a central pipe while cool gas is issued upward from a coaxial pipe that penetrates the particle recovery tank. The swirling motion within the channel is driven by a separated gas flow issued into it uniformly and tangentially through a belt-shaped nozzle region that encircles the chamber wall. The figure includes the numerical results of the flow field in a plane through the axis along with typical particle trajectories in it for large and small particles, i.e. particle size $d_p = 80$ and 20 μm, respectively. Although heat exchange pattern of this type can be more counter-like, the particle recovery efficiency was found to be poor due to the weak downward gaseous motion so that this type was finally abandoned.

Fig. 4 illustrates a bird's eye view of the finally adapted structure. Hot particles are supplied into the cyclone chamber from above through a central pipe while cool gas is introduced into it through a peripheral nozzle that encircles the chamber. The chamber consists of three parts, an upper cylinder, a lower cylinder and a conical part to which a particle recovery tank is connected. The gap of width W between two cylinders forms a nozzle entrance region so that a step on the inner wall between two cylinders corresponds to the nozzle exit position. Twelve helical guide vanes are installed in the entrance region, dividing it into 12 peripheral subchannels. They ensure peripheral uniformity of the gas

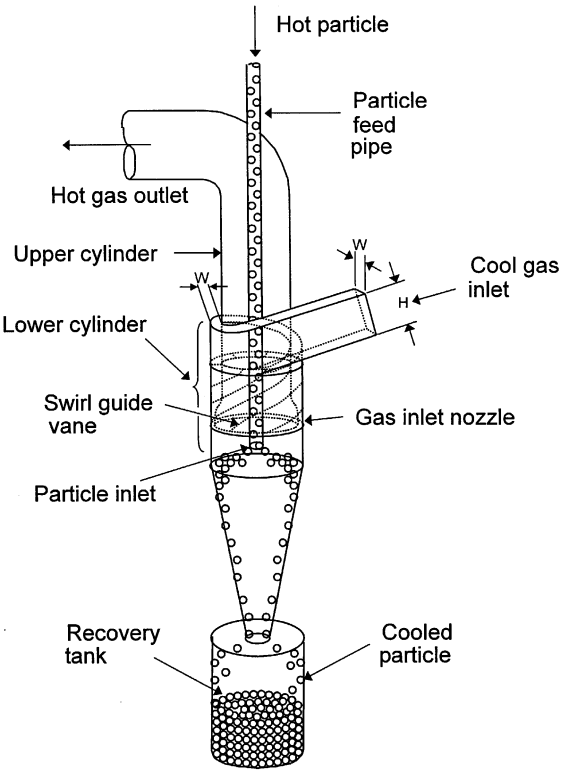

Fig. 4. Bird's eye view of adapted structure.

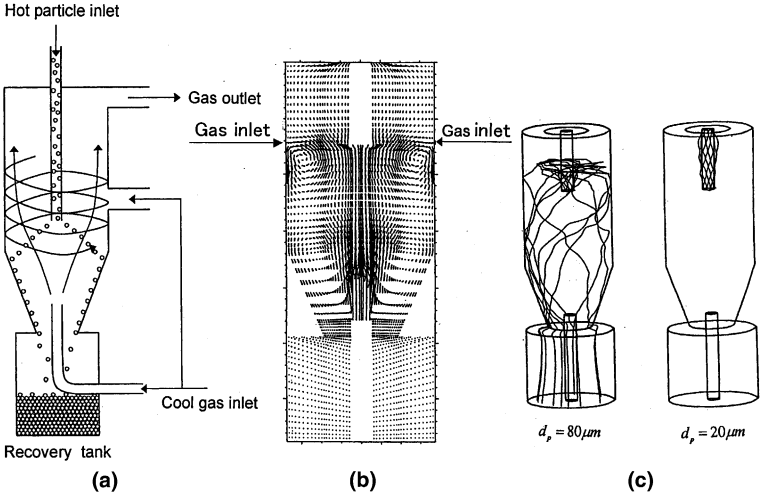

Fig. 3. Example of trial (upward gas issuing): (a) concept; (b) flow field in the plane through axis; (c) typical particle trajectories.

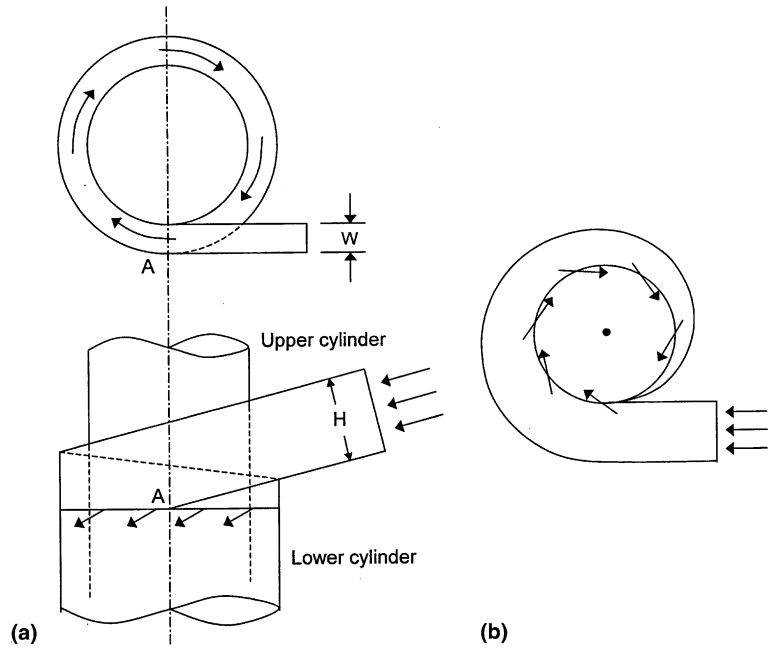

Fig. 5. Volute casing: (a) present case; (b) radial flow turbo machine.

issuing and, simultaneously, give the inlet gas velocity axial as well as peripheral components but no radial component so that they make a strong downward swirl within the chamber.

Another key is the uniformity of inlet flow rate distribution over the 12 sub-channels. For this purpose, the approach duct to the gas inlet is connected obliquely to the nozzle entrance as shown in Fig. 4 and (a) of Fig. 5. It has a square cross-section of width W and height H and is connected tangentially towards the gap between upper and lower cylinders at point A and is twined around it thereafter. Then, the channel height H decreases linearly from H at point A to zero as it turns back to A as shown in (a) of Fig. 5. This linear reduction in H ensures the peripheral uniformity of the inlet gas flow rates over 12 sub-channels. This configuration is similar to the snail-like volute casing of the radial flow turbo machines. The difference is that the present linear decrease in the cross-section occurs in a cylindrical surface around the chamber, while it occurs in a plane normal to the axis in case of the radial turbo machines as in (b) of Fig. 5.

4. Flow and heat exchange patterns

The flow field within the chamber is schematically illustrated in Fig. 6. The swirling gas first goes down along the chamber wall and, then, turns upward near the bottom of the conical part because the particle recovery

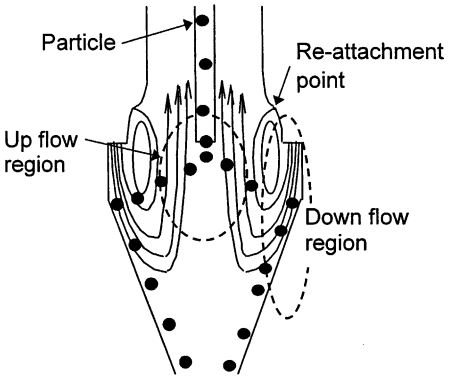

Fig. 6. Schematic of flow field.

tank has no exit for the gas. Then, the flow goes upward in the central part so that a recirculating region is formed along the wall below a certain reattachment point above the nozzle position. Meanwhile, the high temperature particles supplied from the central pipe move outward due to the centrifugal force of the swirl. They also receive drag force from the upward gas flow in addition to the downward gravity so that the particle's outward motion is determined by their balance as well as by particles' initial conditions at the inlet. It is considered, therefore, that the particle that reaches well to the recirculating region, i.e. to a streamline through the reattachment point, will be recovered successfully into

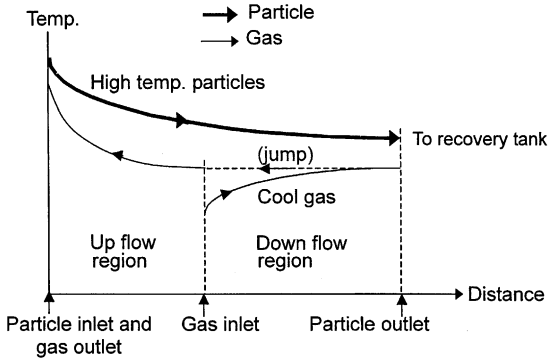

Fig. 7. Heat exchange pattern.

the tank. Otherwise, it will be entrained into the upward flow and will not be recovered. Therefore, the particle recovery efficiency will be higher when the particle motion is more downward.

The heat exchange pattern in the chamber is divided, therefore, into two phenomena. The particles just after being released into the chamber exchange heat with the upward gas flow in "quasi counter-flow" fashion. The more upward the particle motion after releasing is, the more "parallel-like" the heat exchange pattern becomes, while the more downward it is, then, the more "counter-like" the heat exchange pattern becomes. Therefore, the more downward particle feeding seems to be better from the viewpoints of both heat exchange and recovery. However, the problem is not so simple, which will be explained later.

Meanwhile, the particles that have successfully reached the recirculating region exchange their remaining heat with the downward cool gas flow from the nozzle in a purely parallel fashion. The situation is schematically illustrated in Fig. 7. Although the total heat exchange pattern is not purely counter-like, it is considered that the effective recovery of thermal energy can be achieved because the gas flow contacts the hottest particles just before leaving the chamber.

The particles that have reached the recirculating zone are easily captured into the recovery tank due to the

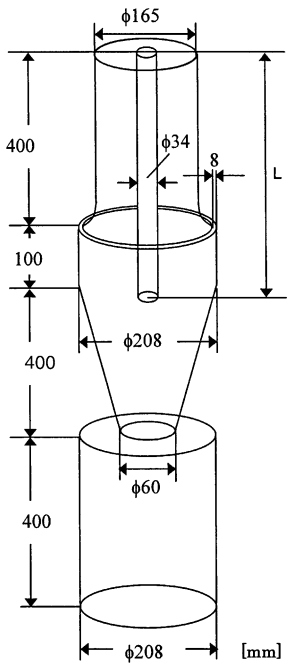

Fig. 8. Adapted dimensions.

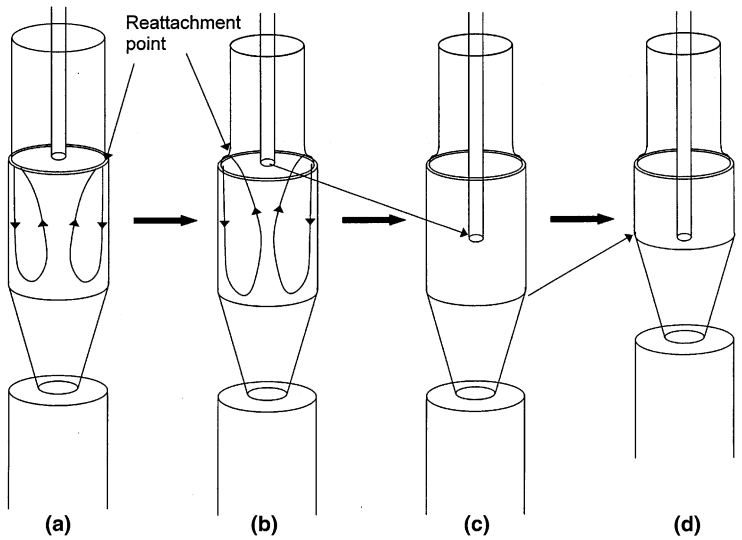

Fig. 9. Process of improvement.

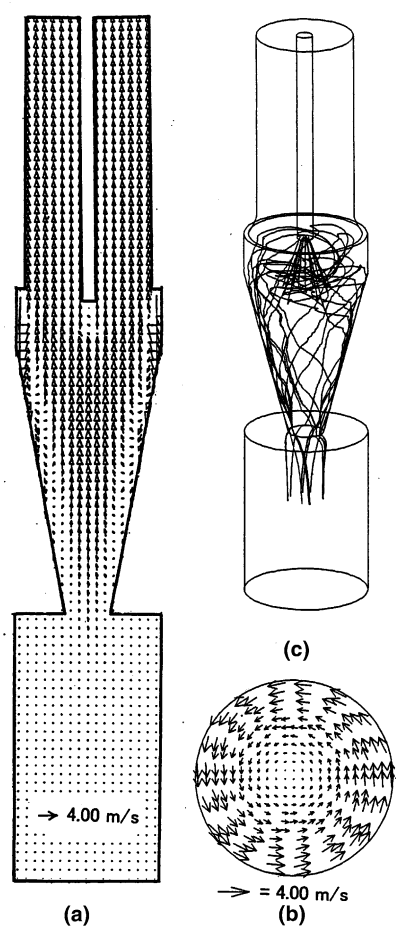

Fig. 10. Gas velocity and particle trajectories for "flush nozzle": (a) gas velocity vector; (b) swirling velocity vector; (c) particle trajectories.

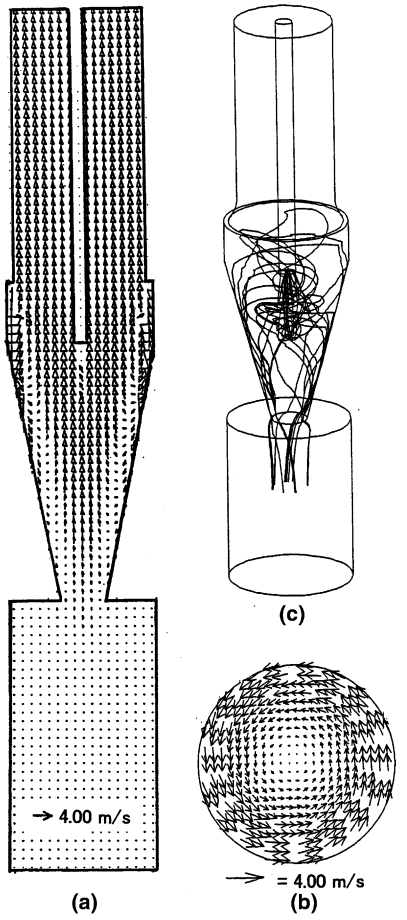

Fig. 11. Gas velocity and particle trajectories for "lower nozzle": (a) gas velocity vector; (b) swirling velocity vector; (c) particle trajectories.

intensified swirl in the conical part as with the usual cyclone separators.

5. Design and manufacturing of a model heat exchanger

After main dimensions were cited from a standard design procedure of conventional cyclone separators, a series of numerical examination was performed in order to confirm the feasibility of the concept and to optimize the details, the main attention being focused on the particle recovery efficiency.

The gas–solid suspension flow field was solved by means of Eulerian/Lagrangian approach. The equations for the gas velocity field were based on the low-Reynolds number version of the k–ε turbulence model proposed by Abe et al. [3]. This model is known to be able to predict correctly the turbulent flows with separation and reattachment. In the preliminary calculations for determining the general shape, the particles were regarded as "passive contaminant" so that the flow fields shown later in Figs. 10 and 11 correspond to the lightly loaded suspensions. Therefore, no source terms were added in the conservation equations for gaseous phase. Also, the particle–particle interaction was neglected for the same reason. The particle used was those of a spherical glass beads with 50 μm diameter and 2520 kg/m^3 material density. This particle was selected as the standard one which the heat exchanger to be designed should successfully recover. Also, the downward inlet velocity of particle was kept at constant value of 1 m/s throughout the calculation while inlet gas velocity was fixed at 8 m/s and its issuing angle to the horizontal was 30°. The turbulent dispersion of each particle was taken into account by means of stochastic method [4]. The particle–wall interaction was assumed to be non-elastic collision where the elastic coefficient and friction coefficient were set at 0.30 and 0.40, respectively.

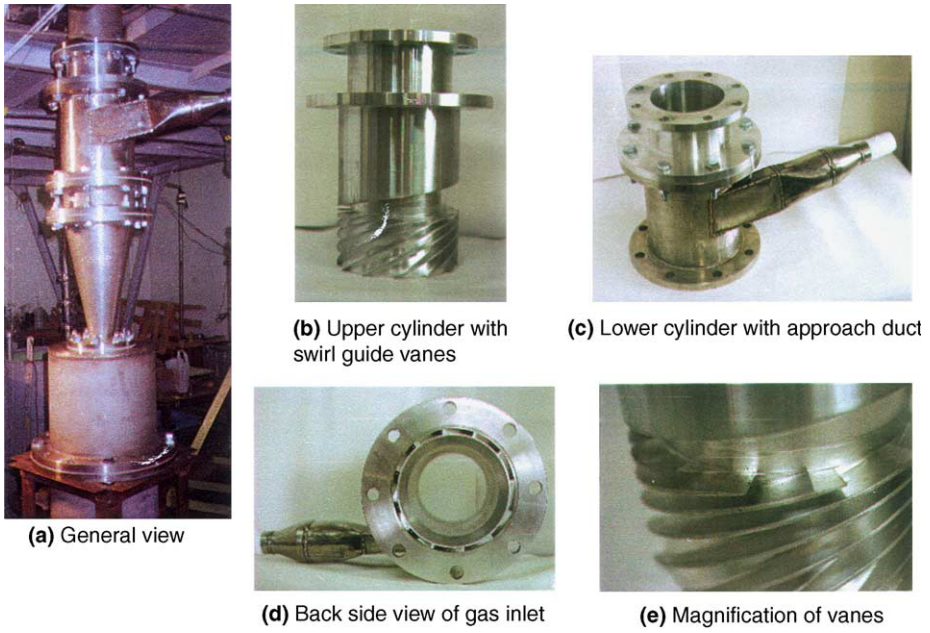

Fig. 12. Model heat exchanger.

The flow field was divided by use of boundary fitted coordinate and the standard division numbers were 25(radial) × 20(peripheral) × 65(axial) in the calculation domain and were delicately adjusted in the process of searching the optimum configuration and dimension of the cyclone.

The finally determined configuration is illustrated in Fig. 8 with some dimensions. The refinement process that derived it was roughly as follows and is illustrated in Fig. 9.

(1) Slight decrease in the inner diameter of the upper cylinder above gas nozzle position which raises the reattachment point and intensifies the swirl there (from (a) to (b)).
(2) Lowering the particle inlet position (from (b) to (c)).
(3) Decrease in the length of lower cylinder as well as the height of the conical part (from (c) to (d)).

Though the numerical results indicated that the lower particle inlet position was superior to the higher case for the effective particle recovery, two particle inlet positions, $L = 500$ and 400 mm in Fig. 8 for each, were examined. They are called hereafter as "lower" and "flush" particle inlet positions, respectively. The word "flush" means that the particle inlet for $L = 400$ mm case is located at the same height as the gas nozzle exit.

Figs. 10 and 11 show the velocity vectors and typical particle trajectories for flush and lower particle inlet positions, respectively. The swirling velocity vectors are those at the location at 20 mm below the particle inlet. The recirculating zone is seen on the wall side but the reattachment point is very close to the gas nozzle. After being released downward, particles go upward to a certain extent due to the upward central gaseous flow and move, at the same time, outward due to the swirl. They are finally recovered into the tank along the near wall region.

Following the numerical verification, a model heat exchanger was manufactured which is shown in Fig. 12. Because the structure of the gas inlet part is very complex, an assembly of the upper cylinder, 12 guide vanes

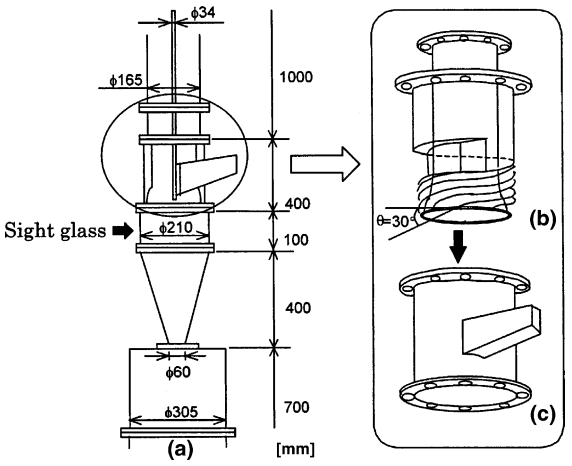

Fig. 13. Combining two cylinders.

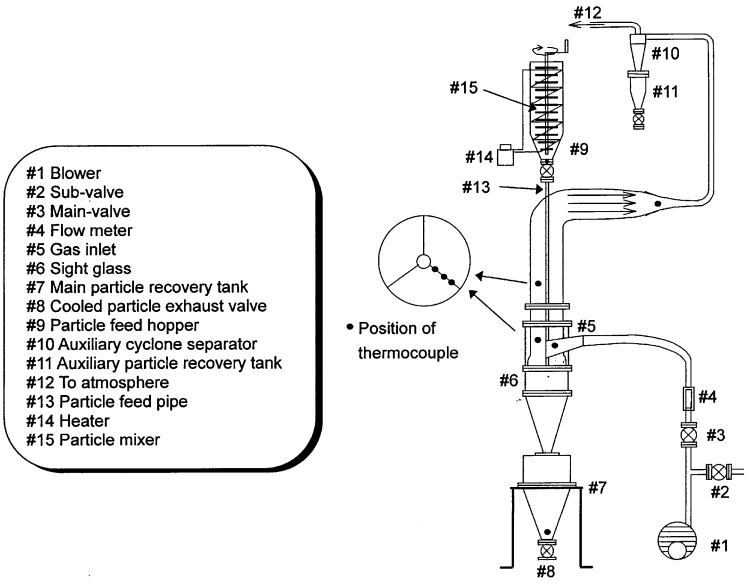

Fig. 14. Experimental system.

and two flanges attached to it was carved out from a single aluminum circular rod by use of NC lathe. It was inserted into the sheath-like lower cylinder part to which the square approach duct was welded in advance. They were connected each other by the flange to form the nozzle and its entrance region, as seen in Fig. 13. The second flange of the upper cylinder was used to connect it to the upper (downstream) structure. A part of the lower cylinder was made of Pyrex glass for visual observation.

The model apparatus was build up into the experimental system shown in Fig. 14. It includes a blower, an adjusting valve, a flow meter, particle feed system, a main recovery tank, an auxiliary cyclone separator and an auxiliary recovery tank, etc.

Table 1
Parameters related to particles

Particle	Material density (kg/m^3)	Average diameter (μm)	Particle response time (s)
Glass beads	2520	44.0	1.8×10^{-2}
		51.2	2.0×10^{-2}
		65.4	3.3×10^{-2}
		77.8	4.7×10^{-2}
		88.4	6.1×10^{-2}
Glassy carbon	1500	10.7	0.11×10^{-2}

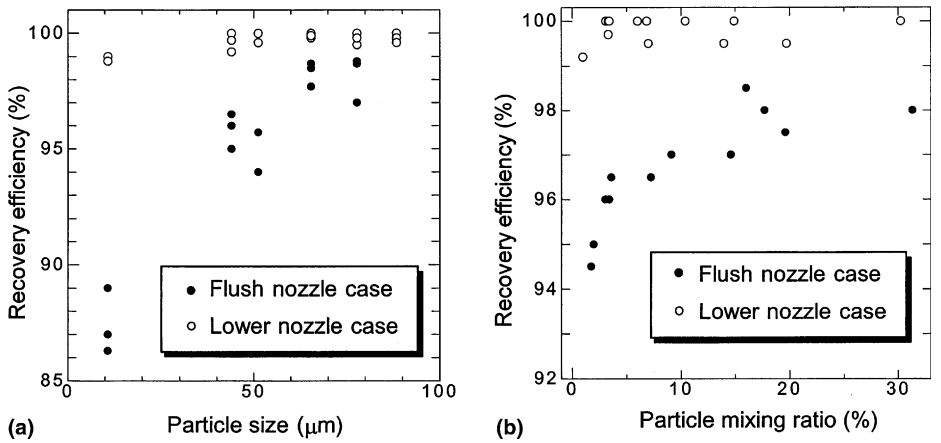

Fig. 15. Particle recovery efficiency.

6. Particle recovery efficiency

First, a series of measurement was performed on the particle recovery efficiency. It is defined as the weight percentage of particles that are successfully captured into the main particle recovery tank to the total feeding amount. The particles used for this are summarized in Table 1. The measurement was first done for small particle mixing ratio less than 5% in which particles are considered to have no substantial effects on the gas flow field. The gas flow rate was fixed at 3.2×10^{-2} kg/s that corresponds to the issuing velocity of 11.6 m/s. The first result is shown in Fig. 15(a) in which the recovery efficiency is plotted vs. particle size. Almost perfect recovery is realized for the lower nozzle position while it is slightly worse for the flush nozzle case especially for smaller particles as is expected.

Fig. 15(b) shows the second result of the recovery efficiency in which the particle mixing ratio is varied for both nozzle positions, the particles being those of 47.6 μm glass beads. For the lower nozzle case, almost perfect recovery is realized irrespective of the mixing ratio while, for the flush nozzle position, the higher recovery efficiency is obtained as the solid mixing increases. However, the visual observation through the sight glass revealed that, for higher mixing ratio, the cloud of particles issued from the feed pipe fell down straightly and collectively without sufficient dispersion. Together with the lower nozzle case, it was anticipated that the excellent recovery efficiency observed for higher mixing would be rather unwelcome in view of the heat exchange performance.

7. Numerical simulation for higher mixing ratio

The previous results suggest that the flow field of higher mixing may be fairly different from that of slight

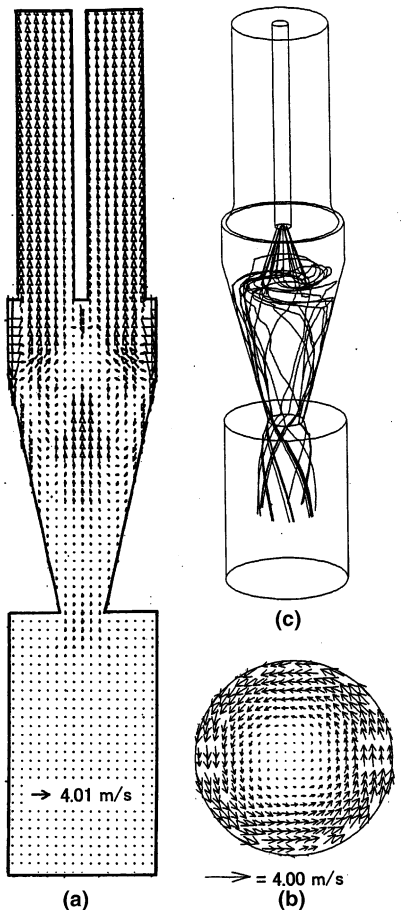

Fig. 16. Flow field and particle trajectories for higher mixing, "flush nozzle": (a) gas velocity vector; (b) swirling velocity vector; (c) particle trajectories.

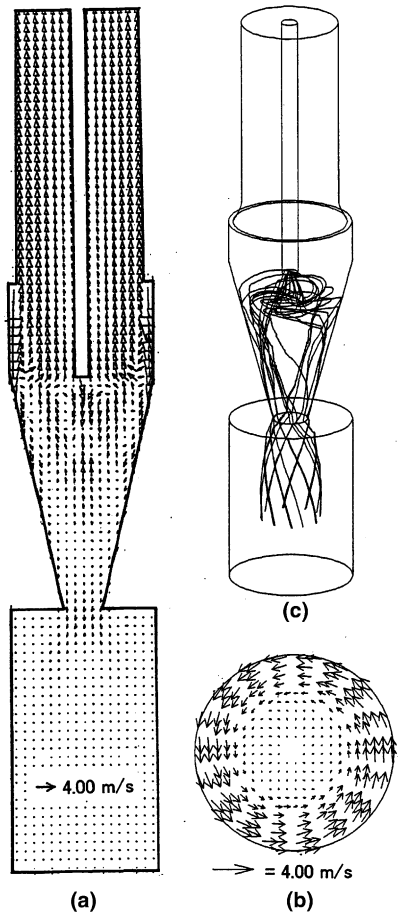

Fig. 17. Flow field and particle trajectories for higher mixing, "lower nozzle": (a) gas velocity vector; (b) swirling velocity vector; (c) particle trajectories.

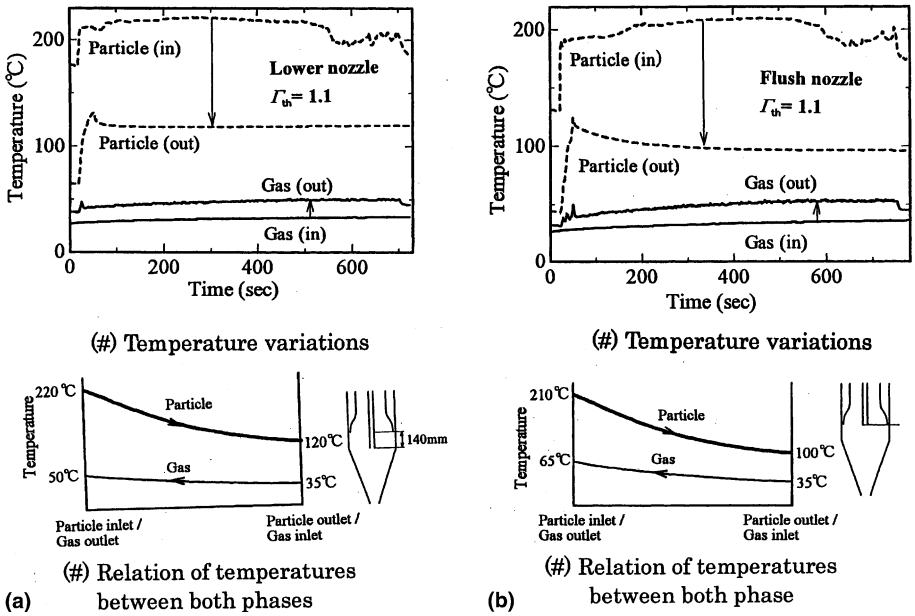

Fig. 18. Experimental results of heat exchange: (a) lower nozzle case; (b) flush nozzle case.

mixing. In the situations where this kind of gas–solid heat exchanger is required, the particle mixing ratio of near unity is important because the best performance of the counter-flow heat exchanger is realized when the heat capacity flow rates of both fluids are of the same order so as to maximize both of the temperature decrease in the primary flow and its increase in the secondary flow. Meanwhile, the particle mixing ratio in the experiment was restricted below 0.5 by feed hopper's capacity. Therefore, the flow field for the mixing ratio of unity was examined again by use of numerical simulations. In this case, the bulk inertias of both phases are equal and the problem must be that of two-way coupling in which gas and particles affect each other. Examined particles were those of glass beads with 50 μm diameter while inter-particle collisions were not considered.

Figs. 16 and 17 show the results in which velocity fields as well as the particle trajectories are illustrated in the same manner as before. Compared to the previous case in which particles were passive contaminant, upward entrainment of the particles has almost disappeared and they are falling downward in more collective manner and the radial particle dispersion occurs at more downward location than in the previous case. On the other hand, the downward gas from the nozzle turns its direction earlier than the light mixing case, avoiding the densely dispersed region of particles so that the gas in the bottom region is almost stagnant. This is also seen in the swirling velocity field in which strong swirl appears only in the near wall region while the central gaseous flow field is almost left stagnant. It must be due to the large specific inertia moment of the particles' cloud just below the particle inlet, which suggests that the heat exchange performance would become poor in spite of the excellent recovery efficiency.

As a temporary summary, it is concluded that good particle recovery efficiency is always guaranteed even for small particles and for higher mixing ratio and it is insensible to the nozzle position. However, the excellent recovery efficiency is rather due to the poor radial dispersion of particles so that it would be unfavorable for the effective heat exchange.

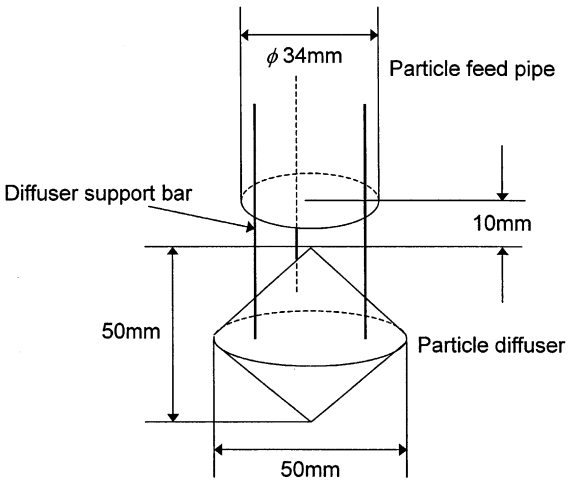

Fig. 19. Particle diffuser.

8. Heat exchange performance

In the heat exchange experiment, a certain amount of preheated particles were charged into the feed hopper and its temperature was kept constant and homogeneous by use of a heater and a mixer. Then, they were dropped into the chamber through valve and feed pipe and exchange their heat with the gas flow. Whole apparatus was wrapped with thermal insulation. The temperatures of inlet and outlet of both phases were recorded by thermocouples. Because of the limited capacity of the feed hopper, the measurement was done in a batch system so that the heat exchange performance was evaluated from the time variation of the temperatures. Particles used were those of spherical glass beads with 56 μm average diameter. The temperature within the feed hopper was kept at 210–220 °C while the inlet air temperature was 30–35 °C. Gas flow rate was fixed at 3.1×10^{-2} kg/s that corresponds to 12 m/s nozzle exit velocity and the particle flow rate was adjusted so as to keep the thermal mixing ratio Γ_{th} at 1.1–1.2. The measurement was performed also for both flush and lower nozzle positions.

Fig. 18(a) shows the results of the lower nozzle case in which time variation of the inlet and outlet temperatures of both phases and their relations are illustrated. Although the heat balance is not necessarily good, i.e. about 25% heat is lost to the heat capacity of the apparatus; the gaseous outlet temperature does not come up to the outlet temperature of the particles so that

Fig. 20. Particle dispersion after feeding: (a) without diffuser; (b) with diffuser.

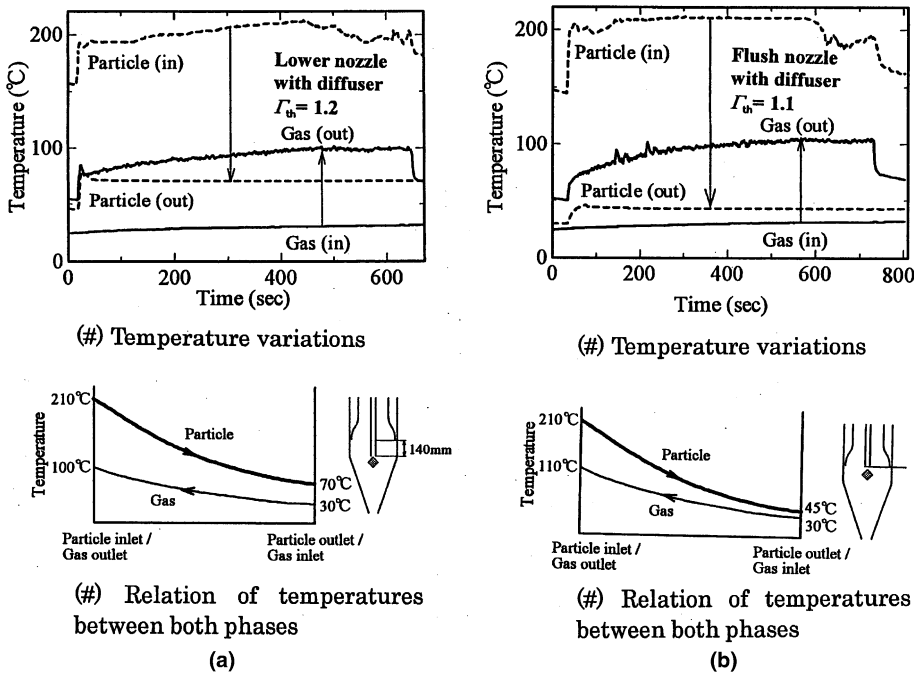

Fig. 21. Experimental results of heat exchange with diffuser: (a) lower nozzle case; (b) flush nozzle case.

the goal of the present study has not been achieved. Fig. 18(b) is the same results of the flush nozzle case. Although a slight improvement is recognized, the general trend is unchanged. The slight improvement itself is considered to be simply due to the increased path length along which heat exchange is done. Meanwhile, the particle recovery efficiency was almost 100% for both cases.

9. Particle diffuser

The reason for the observed poor heat exchange performance is considered as follows. The cloud of particulate phase has much larger specific inertia than the gaseous phase for higher density case while the centrifugal force acting on a particle is exactly zero at the centerline so that the particles densely supplied from the feed pipe fall down straightly to the recovery tank without moving outward, which interferes the effective heat exchange. To prevent it, a small top-shaped particle diffuser was hanged just below the particle inlet, as shown in Fig. 19 in order to promote the dispersion into radial direction. Once the particles move outward

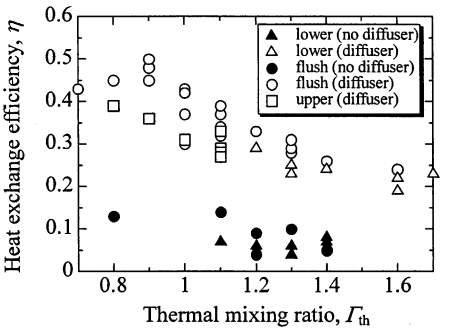

Fig. 22. Heat exchange efficiency.

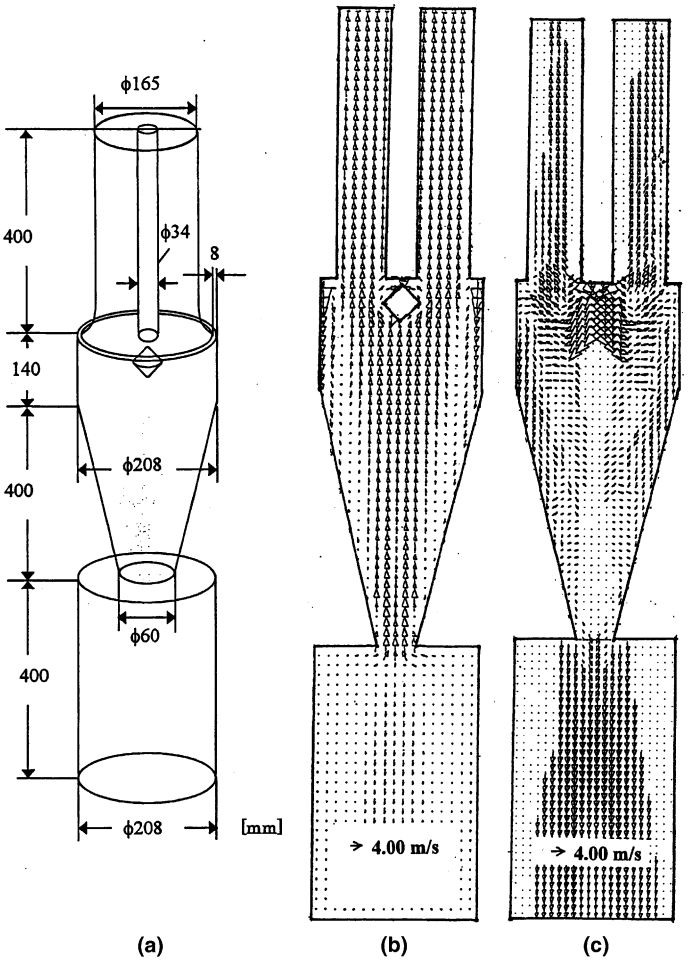

Fig. 23. Flow field with particle diffuser.

slightly, they receive the centrifugal force well so that the effective dispersion and heat exchange would be realized. Fig. 20 reveals the situation observed through the sight glass.

The results with the diffuser are summarized in Fig. 21. The outlet temperatures of the gas are seen to exceed those of particles so that the original goal has been finally achieved. It is also seen that the flush nozzle case is slightly superior to the lower nozzle case. The reason may be that for the lower nozzle case the ratio of the gas flow that turns upward without exchanging heat with particles is larger than for the flush nozzle case. An attempt was also made to raise the particle inlet position 100 mm above the gas outlet but the heat exchange efficiency became rather worse. The particle recovery efficiency over 98% was always obtained even in the case with particle diffuser.

Fig. 22 summarizes the heat exchange efficiency defined as the ratio of the heat recovered by gas to the heat supplied by particles, the abscissa being the thermal mixing ratio. It is found that the best configuration is the flush nozzle position with diffuser.

Figs. 23 and 24 show the numerical results of the flow and temperature fields with the diffuser for the flush nozzle position, other conditions including the mixing ratio being the same as in Fig. 16. As for the temperature field of Fig. 24, the result without the diffuser is also shown for comparison. It is found that too early reflection of the gas flow observed before has been disappeared and the gas is going out with sufficiently elevated temperature while particles are being captured into the recovery tank with sufficiently low temperature. The inlet/outlet bulk temperatures of both phases evaluated by the simulation with the diffuser were 210/46 °C

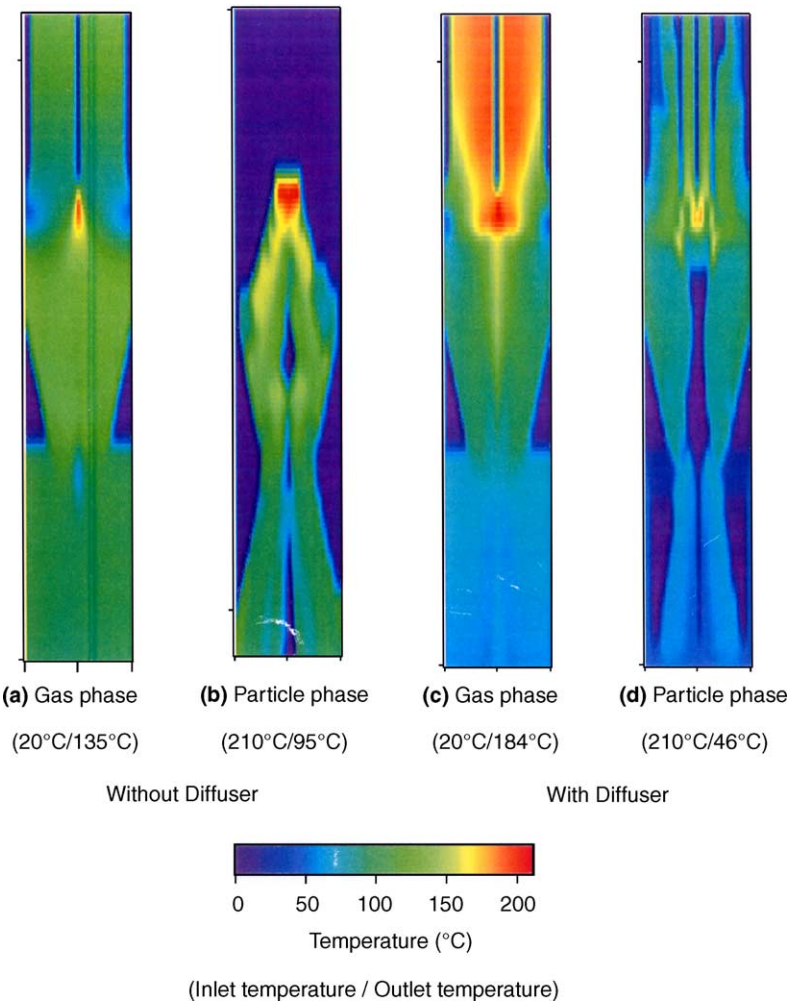

Fig. 24. Temperature fields of both phases.

for particles and 20/184 °C for gas, respectively, while they were 210/95 °C for particles and 20/135 °C for gas without the diffuser.

10. Summary

Motivated by the requirement of equipment for the effective recovery of thermal energy carried by particulate or granular materials, a direct contact gas–solid heat exchanger by use of an axial flow cyclone was developed. The key is to make a flow field in which gas and solid particles move in a manner of near counter-flow. After going through a series of numerical experiments, a prototype form of the heat exchanger was determined in which heat receiving gas is issued into the chamber in downward axial direction, making a strong swirl within it, while particles of high temperature are fed at the center of the cyclone from above, which is in contrast to conventional cyclone separators. More numerical simulations were carried out in order to achieve good performance and a model heat exchanger was made based on them. According to the measurement by use of it, almost perfect recovery efficiency of particles was always obtained irrespective of mixing ratio, particle size and particle inlet position. However, the heat exchange performance was found to be poor in its original form. According to both numerical examination and visual observation of the flow field, the reason for this was attributed to an insufficient radial dispersion of particles due to their large specific inertia. Following this, a small particle diffuser was attached just below the particle inlet in order to prompt the dispersion. The effect of attaching the diffuser was remarkable, bringing about a drastic improvement in the heat exchange performance. The gaseous outlet temperature much higher than the particle outlet temperature was finally obtained both experimentally and numerically, which is never realized in the case of parallel flow heat exchange or in the cooling by the simple gas–solid mixing.

Acknowledgements

The original motivation of this study can be traced back to a stimulation given to one of the authors in his school years by Prof. R. Echigo. His fountain of knowledge and idea was exiting and fruitful from which many students including him were always receiving fresh incentives and being encouraged.

References

[1] S. Mori, H. Miura, T. Suzuki, A. Shimizu, Y. Seki, T. Kunugi, S. Nishio, N. Fujisawa, A. Hishinuma, M. Kikuchi, Preliminary design on a solid particulate cooled blanket for the steady state Tokamak reactor, Fusion Technol. 21 (1992) 1744–1748.

[2] S. Yamasaki, H. Miura, H. Koike, Y. Seki, T. Kunugi, S. Nishio, I. Aoki, A. Shimizu, Design study of helium-solid suspension cooled blanket and divertor plate for a Tokamak power reactor, Fusion Eng. Design 25 (1993) 227–238.

[3] K. Abe, T. Kondoh, Y. Nagano, A new turbulence model for predicting fluid flow and heat transfer in separating and reattaching flows, Int. J. Heat Mass Transfer 37 (1994) 139–151.

[4] T. Yokomine, A. Shimizu, Prediction of turbulence modulation by using k–ε model, Advances in Multiphase Flow, Elsevier Science, The Netherlands, 1995.